Chemical Geology 280 (2011) 170–179

Contents lists available at ScienceDirect

Chemical Geology

journal homepage: www.elsevier.com/locate/chemgeo

Iron isotope fractionation during biogeochemical cycle: Information from suspended particulate matter (SPM) in Aha Lake and its tributaries, Guizhou, China

Liuting Song [a,b,c], Cong-Qiang Liu [a,*], Zhong-Liang Wang [a], Xiangkun Zhu [c], Yanguo Teng [b], Lili Liang [a], Suohan Tang [c], Jin Li [c]

[a] State Key Laboratory of Environmental Geochemistry, Institute of Geochemistry, Chinese Academy of Sciences. Guiyang 550002, China
[b] College of Water Sciences, Beijing Normal University, Beijing 100875, China
[c] Institute of Geology, Chinese Academy of Geological Sciences, Beijing 100037, China

ARTICLE INFO

Article history:
Received 5 November 2009
Received in revised form 1 October 2010
Accepted 4 November 2010
Available online 11 November 2010

Editor: B. Bourdon

Keywords:
Iron isotope
Suspended particulate matter
Lake
River

ABSTRACT

Iron isotope compositions of suspended particulate matters (SPM) collected from the Aha Lake, an artificial lake in the karst area of Yun-Gui Plateau, and its tributaries in summer and winter were investigated for our understanding of the behavior of Fe isotopes during iron biogeochemical cycling in lake. δ^{56}Fe values of SPM display statistically negative shift relative to IRMM-014. Samples from the lake display a range from −1.36‰ to −0.10‰ in summer and from −0.30‰ to −0.07‰ in winter, while river samples vary from −0.88‰ to 0.07‰ in summer and from −0.35‰ to −0.03‰ in winter. The average iron isotope composition of aerosol samples is +0.10‰, which is very similar to that of igneous rocks (0.09‰). The SPM in most rivers and water column showed seasonal variation in δ^{56}Fe value: the δ^{56}Fe values of SPM in summer were lower than in winter. The seasonal variation in δ^{56}Fe value of the riverine SPM should be ascribed to the change in source of particulate Fe and geochemical process in the watershed: More particulate Fe was leached from soil and produced by weathering of pyrite widely distributed in coal-containing strata. It is suggested that both allochthonous inputs and the redox iron cycling control the variations of δ^{56}Fe values for SPM in lake.
During summer stratification, an Fe cycle named "ferrous wheel" is established near the redox boundary where the upwardly diffusing Fe(II) is oxidized and the reactive Fe oxides formed will continuously sink back into the reduction zone to complete the cycle. The δ^{56}Fe values for SPM reach the minima, −0.88‰ for DB station and −1.36‰ for LJK station, just near the redox boundary as a result of the Fe cycling, where a rough 45% to 76% of Fe in these particles was produced by the repetitive cycle. Due to random transportation and diffusion, δ^{56}Fe values of the particles near the redox zone distributed into approximately a Gaussian shape. The good negative correlation existed between δ^{56}Fe values and Fe/Al ratios for DB station, suggesting that they together can be used as good indicators of the redox-driven Fe transformations.

1. Introduction

As the fourth most abundant element in the Earth's crust, iron is of great importance in the surface and sub-surface environments. The extremely low concentration of iron in modern oceans has been thought to be responsible for the low primary production in the High Nutrient, Low Chlorophyll zone (e.g., Coale et al., 1996; Martin et al., 1991). Therefore, iron may play an important role in regulating the atmospheric CO_2 and even the climate change (Martin, 1990), and hence the biogeochemical cycling of iron at the Earth's surface and sub-surface environments draws intense attention to scientists. In lakes, iron is also thought to have an influence on the algal growth (Clasen and Bernhardt, 1974; Evans and Prepas, 1997). There are a variety of sources of iron for lake water, such as tributary inputs, autochthonous material (material produced during primary production and mineralization), sediment resuspension, and atmospheric depositions (Håkanson and Peters, 1995; Malmaeus and Håkanson, 2003). The fate and transport of iron strongly depends on the reactions involving iron, including biological and abiological processes, and these reactions make the biogeochemical cycling of iron complicated.

Iron isotopes have been shown to be fractionated during a number of processes, and they can be potentially used for identifying and quantifying these processes, especially after the improvement of analytical techniques with better than 0.1‰ (2SD, two standard deviations) reproducibility (reviews: Beard and Johnson, 2004; Johnson et al., 2004; 2008). Most studies have been done on compositional variations and fractionation of iron isotopes in rivers, oceans and soil systems (Zhu et al., 2000; Rouxel et al., 2004; Emmanuel et al., 2005;

* Corresponding author. Fax, +868515891609.
E-mail address: liucongqiang@vip.skleg.cn (C.-Q. Liu).

0009-2541/$ – see front matter © 2010 Elsevier B.V. All rights reserved.
doi:10.1016/j.chemgeo.2010.11.006

Staubwasser et al., 2006; Ingri et al., 2006; Bergquist and Boyle, 2006; Fehr et al., 2008; Poitrasson et al., 2008; Severmann et al., 2006; 2008; 2010), whereas relatively less research has been done on lakes (Malinovsky et al., 2004; Teutsch et al., 2009). Accordingly, there is still so much work to be completed before we can successfully use iron isotope to unravel biogeochemical cycling of iron. Lakes are easily accessible natural laboratories as there are a series of biogeochemical processes involved. This study focuses on Aha Lake, which is a seasonally anoxic artificial lake located on the southwest suburb of Guiyang, Guizhou Province, China. Iron isotopic compositions of suspended particulate matters in lake water and the tributaries were mainly investigated to assess the behaviors of iron isotopes during biogeochemical cycling in summer and in winter.

2. Study site, sampling and analytical details

2.1. Study site

Aha Lake is a seasonally anoxic lake located in the suburb, about 8 km southwest of Guiyang, China (Fig. 1), with a surface area of 4.5 km^2 and a total volume of 5.4×10^8 m^3. The average and maximum depths are 13 m and 24 m, respectively. The retention time of lake water is about 0.44 year. The watershed area is 190 km^2 with an average annual precipitation of 1109 mm and an average annual evaporation of 932 mm, and the average annual temperature is 15.3 °C.

The bedrock is mainly a mixture of Permian carbonate rock and coal-bearing strata covered with silico-alumina and silico-ferric yellow soil in the watershed area of Aha Lake. There are also small amounts of outcrops of Triassic carbonate rock covered with black and tan limestone soil. Previously, more than 200 coal mines were widely distributed in the watershed, where significant amount of acid mining drainages and dump filtrates were produced. There are mainly six rivers flowing through the watershed area including five inflowing tributaries, Youyu River (YR), Caichong River (CR), Lannigou River (LR), Baiyan River (BR) and Sha River (SR), and only one discharging river, Xiaoche River (XR) (Fig. 1). YR, CR and LR are the main tributaries for LJK station while BR and SR are for DB station. Their water discharges are shown in Fig. 1. Within these rivers, YR, CR and BR are seriously contaminated due to acid mining drainages. Lime added at upstream sites along these rivers moderates the solution pH but deteriorates the hardness of water.

2.2. Sampling

All the wares used in laboratory and in field were carefully cleaned. Polyethylene bottles, tubes and HDPE bottles for sample collections were all soaked with 6 N HCl (GR) for more than three days and then rinsed with 18.2 MΩ Milli-Q water. The filters (Millipore HA, 0.45 μm, 47 mm) were treated three times with 1 M double-distilled HCl, alternating with 18.2 MΩ Milli-Q water. The brown glass bottles were firstly acid cleaned and then combusted, together with the glass microfiber filters (Whatman, GF/F, 25 mm) used for dissolved organic carbon (DOC) samples, in the muffle furnace at 450 °C for 4 h.

Sampling in Aha Lake was performed at two stations, Liang Jiang Kou (LJK) at the upstream site and Da Ba (DB) at the downstream site. River water samples were collected for all the five main inflowing rivers at downstream sites and XR for the outflow water near the Dam. Water sampling was performed in July and August of 2006 (summer) and January of 2007 (winter). Bottles for sampling were pre-rinsed with the corresponding water samples for three times. A multi-parameter sensor was used for determining the pH, water temperature (T), electrical conductivity (EC), and dissolved O_2 (DO). Samples for measurement of dissolved Fe, Mn and Al were filtered with 0.45 μm membrane filter in field and filtered samples were acidified to pH<2 with ultra pure HNO_3. Separated samples were also filtered for DOC with glass microfiber filters and glass syringe in field. All the samples were stored in refrigerator at 4 °C before analysis. Fe, Mn and Al were analyzed on Inductively Coupled Plasma-Optical Emission Spectrometry (Varian Vista MPX). DOC concentrations were analyzed on TOC (OI Analytical Aurora Model 1030).

Samples for the measurements of iron isotopic compositions were filtered through 0.45 μm Millipore HA membrane filters. The filters with SPM were stored in polyethylene tubes in refrigerator. Aerosol samples were collected with a homemade polyethylene rainwater sampler. The rainwater was filtered immediately after sampling and the filters with aerosol particles were stored in refrigerator.

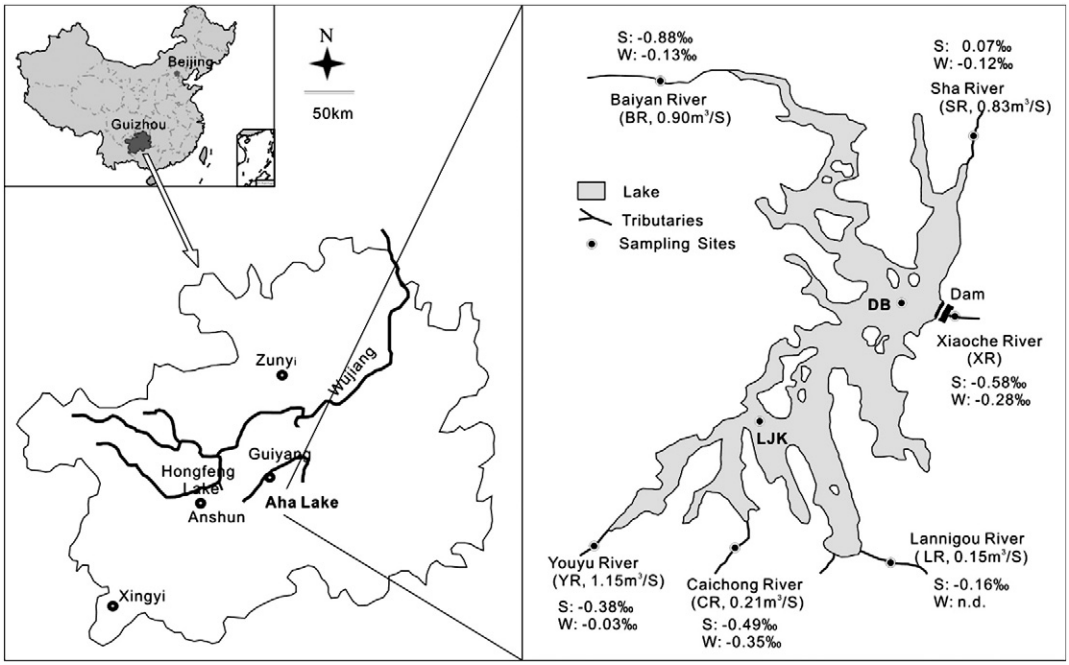

Fig. 1. Location map of Aha Lake, southwest China. Shown together in the map are its main tributaries, discharges of the inflowing rivers and the sampling sites. δ^{56}Fe values of the inflow and outflow rivers were also summarized in this figure, where S stands for summer and W for winter.

2.3. Iron isotope analysis

The sample preparation work was carried out in clean room. All the critical work including sample dissolution and purification was completed in class 100 laminar flow hoods. Hydrochloric acid was distilled twice in quartz sub-boiling still and hydrofluoric acid and nitric acid were distilled with Teflon two-bottle setups. The Milli-Q water (18.2 MΩ) was used throughout the procedures.

2.3.1. Sample dissolution

All the lake and river SPMs and aerosol samples were firstly dried at 50 °C in an oven, the interior of which was covered with Teflon materials. These samples were then soaked with 3 ml aqua regia and 0.5 ml concentrated HF for 48 h in acid-cleaned Teflon beakers (7 ml, Savillex). The beakers were left on the hot plate and dried at 80 °C. Another 3 ml aqua regia and 0.5 ml concentrated HF were added and the closed beaker was left on the hot plate for 72 h at 140 °C. The procedure was repeated until the particles were thoroughly digested. If necessary, the distilled $HClO_4$ was used to facilitate the digestion. The digested samples were left on the hot plate to dryness at 80 °C and the procedure was sequentially repeated for three times with 0.5 ml concentrated HCl to eliminate HNO_3 and HF. Finally, each sample was redissolved into 7 N HCl + 0.001%H_2O_2 for chemical purification.

2.3.2. Chemical purification

Chemical purification was carried out using procedures similar to that of Maréchal et al. (1999) and Tang et al. (2006), with slight modifications. Details are described as follow: Anion-exchange chromatography was performed with polypropylene column (Bio-Rad, diameter: 6.8 mm, height 4.3 cm) filled with AG MP-1 resin (Bio-Rad, 100–200 mesh, chloride form). The resin was firstly cleaned with 2 ml 0.5 M HNO_3 alternating with 10 ml 18.2 MΩ Milli-Q water for three times. Then 5 ml Milli-Q water was used to ensure that the HNO_3 was thoroughly removed. The resin was then continuously pre-conditioned with 5 ml 7 N HCl + 0.001%H_2O_2 and 4 ml 7 N HCl + 0.001%H_2O_2. After loaded with the prepared samples, the matrix were striped with 35 ml 7 N HCl + 0.001%H_2O_2 and Fe was eluted with 20 ml 2 N HCl + 0.001%H_2O_2. The Fe eluate was evaporated to dryness with one drop of concentrated H_2O_2 on a hot plate at 80 °C. All the samples were purified twice to make sure that Fe was separated from the matrix elements. Finally, the purified Fe was redissolved three times with 0.1 ml concentrated HNO_3 and evaporated to dryness to drive off the chloride ions. The final Fe eluate was dissolved in 1% HNO_3 with a concentration of 5 ppm for isotope analysis. The recoveries of Fe for all samples were >95%. The procedural blanks including digestion, column purification and evaporation were always less than 0.34% of the total Fe extracted from the samples.

2.3.3. Mass spectrometry

Iron isotope analyses were performed on a Nu Plasma instrument HR MC-ICP-MS. The Fe samples, with concentrations ranging from 5 ppm to10 ppm in 1% HNO_3, were introduced to the argon plasma via a desolvating nebulizer DSN-100 system. The typical ion beams for 5 ppm Fe solutions of both standards and samples were ca. 18 V on ^{56}Fe and the blanks were always below 0.005 V. The SSB (standard-sample bracketing) method has been used throughout the study to minimize the instrumental mass bias and the standard-sample concentrations matched within 5%. The performance of the instrument was assessed by repetitive measurements of an internal lab standard (CAGS-Fe3) relative to the Fe isotope reference material IRMM-014. The average Fe isotope values for CAGS-Fe3 are $\delta^{57}Fe = 1.23 \pm 0.11‰$ (2SD) and $\delta^{56}Fe = 0.83 \pm 0.08‰$ (2SD) in high resolution mode under optimized conditions. The long-term instrumental reproducibilities defined from the 16 months' replicate analyses are 0.11‰ for $\delta^{57}Fe$ and 0.08‰ for $\delta^{56}Fe$. The detailed operation conditions and the performance of isotope measurements were described in Zhu et al. (2008).

Fe isotope data are reported in $\delta^{x}Fe$ ($\delta^{56}Fe$, $\delta^{57}Fe$) as parts per thousand deviations relative to IRMM-014. All the $\delta^{56}Fe$ and $\delta^{57}Fe$ values obtained in this study followed the theoretical mass-dependent fractionation line, with a formula of $\delta^{57}Fe = 1.4641 \times \delta^{56}Fe\text{-}0.0004$ ($R^2 = 0.9944$).

$$\delta^{x}Fe = \left[\left({}^{x}Fe / {}^{54}Fe \right)_{sample} \Big/ \left({}^{x}Fe / {}^{54}Fe \right)_{IRMM} - 1 \right] \times 1000$$

3. Results

3.1. Environmental parameters and concentrations of selected anions

Environmental parameters are summarized in Table 1 and displayed as a function of water depth in Fig. 2. Due to lower temperature, lake water overturns in winter, resulting in a homogeneous water body (Fig. 2). In summer, thermal stratifications were observed in August and July (summer) with a temperature gradient of ca. 10 °C. The thermoclines were located at a water depth of ca. 10 m for DB station and ca. 6 m for LJK station. The depth-dependent profiles of pH, DO, EC, DOC are shown in Fig. 2. The dissolved oxygen became almost depleted in hypolimnion, with a concentration of 1.6 to 2 mg L^{-1}, and the hypoxic condition prevailed. There was also a marked decrease of pH (0.5–1.2 unit) in the deep strata (Fig. 2). EC value ranges from 500.3 to 685.1 μs cm^{-1}, being high with respect to other fresh lake water, which may be caused by fluvial inputs deteriorated by coal mine drainages and lime addition. Electrical conductivity continuously increases with water depth until there is a sharp decrease of 102 μs cm^{-1} in hypolimnion for especially LJK station. In contrast, DOC concentrations are much higher in summer than in winter especially for surface and near sediment water.

The concentrations of SO_4^{2-}, NO_3^- and Cl^- were also measured for the tributary river and lake water samples. The concentrations of SO_4^{2-} vary within ranges of 0.94 mM to 5.96 mM in the inflowing river water and of 1.91 mM to 2.79 mM in lake water, while the NO_3^- concentrations vary from 0.05 mM to 0.21 mM in the river water and from 0.03 mM to 0.12 mM in lake water. The Cl^- had concentrations of 0.07 mM to 0.63 mM in river water and of 0.25 mM to 0.37 mM in lake water. The river water showed higher SO_4^{2-} concentrations than lake water and the rivers BR and YR that are polluted by coal mine drainage showed the highest SO_4^{2-} concentrations among the studied rivers.

3.2. Dissolved Fe, Mn and Al in the lake and tributary water

The concentrations of dissolved Fe ranged from 0.1 μM to 0.48 μM in the tributary water, and 0.05 μM to 0.51 μM in the lake water in summer (Table 1). Except for one deep water sample of the lake, the lake water had lower contents of dissolved Fe as compared to the tributary river water. The contents of dissolved Mn and Al in river water varied in the range of 0.3 μM to 36.8 μM and 0.75 μM to 3.29 μM, respectively.

The surface water at different stations and in different seasons showed largely variable contents of dissolved Fe, Mn and Al, ranging from 0.06 μM to 0.12 μM, from 0.01 μM to 0.11 μM, and from 0.01 μM to 1.10 μM, respectively. The variations in concentration of these elements along the depth of different water columns were not simple. For LJK station, the surface water had a high dissolved Fe concentration of 0.12 μM in summer, much higher than those of the deep water in summer, but not the case in winter. At DB station, slight increase with depth was displayed for both dissolved Fe and Mn contents until there were strong increases appeared in the near-sediment water in summer (Fig. 3), which were not observed for other stations. Similar to DOC distributions, the concentrations of dissolved Al were higher in summer especially for surface water (Figs. 2 and 3).

Table 1
Environmental parameters and chemical data of lake and tributary water of Aha Lake, southwest China.

Sample station	Date	Depth (m)	T (°C)	pH	DO (mg L^{-1})	EC (μs cm^{-1})	DOC (mg L^{-1})	Fe_d (μM)	Mn_d (μM)	Al_d (μM)	SO_4^{2-} (mM)	NO_3^- (mM)	Cl^- (mM)
DB	Aug 2006	0	25.0	8.19	7.00	533.9	4.54	0.06	0.01	1.10	1.97	0.07	0.32
DB	Aug 2006	−4	25.2	8.32	7.04	536.8	3.64	0.06	<0.01	0.15	2.13	0.07	0.33
DB	Aug 2006	−8	24.6	7.93	5.11	556.3	3.08	0.07	0.02	0.50	2.24	0.08	0.30
DB	Aug 2006	−12	22.3	7.70	5.32	558.0	3.52	0.09	4.13	0.24	2.35	0.07	0.28
DB	Aug 2006	−16	17.4	7.53	2.09	615.6	3.18	0.09	9.31	0.23	2.55	0.06	0.29
DB	Aug 2006	−20	14.9	7.50	1.98	624.3	3.23	0.09	12.70	0.52	2.57	0.05	0.29
DB	Aug 2006	−23	14.6	7.60	2.00	533.1	3.06	0.12	31.45	0.67	2.51	0.04	0.28
DB	Aug 2006	−24					4.88	0.51	94.92	0.21	1.91	0.03	0.23
LJK	Jul 2006	0	30.9	8.35	7.50	628.4	10.26	0.12	0.03	0.46	2.12	0.08	0.32
LJK	Jul 2006	−3	30.6	7.65	7.80	627.4	5.62	0.05	<0.01	0.33	2.24	0.08	0.37
LJK	Jul 2006	−6	30.1	7.46	6.51	680.4	6.75	0.06	0.01	0.96	2.19	0.06	0.29
LJK	Jul 2006	−9	23.0	7.13	2.33	685.1	1.94	0.05	<0.01	0.59	2.79		0.20
LJK	Jul 2006	−13	15.8	7.10	1.65	582.6	8.37	0.06	18.04	0.19	2.61		0.26
LJK	Jul 2006	−14			1.60						2.55		0.25
DB	Jan 2007	0	7.9	7.49	8.43	500.3	2.41		0.11	0.57	2.09	0.12	0.34
DB	Jan 2007	−5	7.4	7.49	7.70	539.3	2.83		0.08	0.52	2.24	0.12	0.32
DB	Jan 2007	−10	7.3	7.97	8.14	534.5	2.62		0.03	0.39	2.27	0.11	0.30
DB	Jan 2007	−15	7.1	7.95	8.76	535.6	2.34		0.02	0.33	2.35	0.11	0.30
DB	Jan 2007	−20	7.2	7.92	8.80	539.7	2.19		0.05	0.17	2.37	0.11	0.30
DB	Jan 2007	−23	7.3	7.90	8.33	539.0	2.15		0.09	0.10	2.39	0.11	0.30
LJK	Jan 2007	0	7.3	7.95	9.00	520.9	2.10		0.05	<0.01	2.41	0.11	0.29
LJK	Jan 2007	−3	7.6	7.80	8.88	521.4	2.28		0.06	<0.01	2.43	0.10	0.29
LJK	Jan 2007	−6	7.6	7.87	8.60	519.6	2.10		0.04	<0.01	2.46	0.11	0.30
LJK	Jan 2007	−10	7.4	7.46	9.20	518.9	2.36		0.03	0.37	2.40	0.11	0.29
YR	Aug 2006	0	21.6	8.18	8.17	901.8	1.96	0.18	15.36	0.82	5.44	0.05	0.07
YR	Jan 2007	0	8.6	7.88	9.28	652.4	1.20		36.78	0.75	4.20	0.07	0.08
CR	Aug 2006	0	21.6	7.66	5.19	646.1	4.01	0.21	0.54		2.40	0.21	0.38
CR	Jan 2007	0	9.3	7.71	8.80	679.0	8.27		2.85	0.90	2.27	0.12	0.46
LR	Aug 2006	0					7.84	0.48	1.64	0.46			
LR	Jan 2007	0	8.7	7.14	5.11	540.5	18.57		1.89	3.29	0.94	0.08	0.52
BR	Aug 2006	0	21.8	8.04	7.47	715.9	2.12	0.16	1.39	1.04	4.02	0.06	0.07
BR	Jan 2007	0	7.4	8.42	10.32	285.0	1.28		0.61	1.03	5.96	0.11	0.13
SR	Aug 2006	0	22.6	8.28	7.60	595.8	6.16	0.16	0.55	4.26	1.20	0.13	0.44
SR	Jan 2007	0	8.7	8.28	10.04	480.1	3.74		0.39	2.09	1.31	0.17	0.63
XR	Aug 2006	0	12.0	7.21	5.19	661.9	2.53	0.10	2.97		2.64	0.06	0.27
XR	Jan 2007	0	7.7	7.66	8.45	538.4	2.14		0.61	0.42	2.36	0.11	0.30

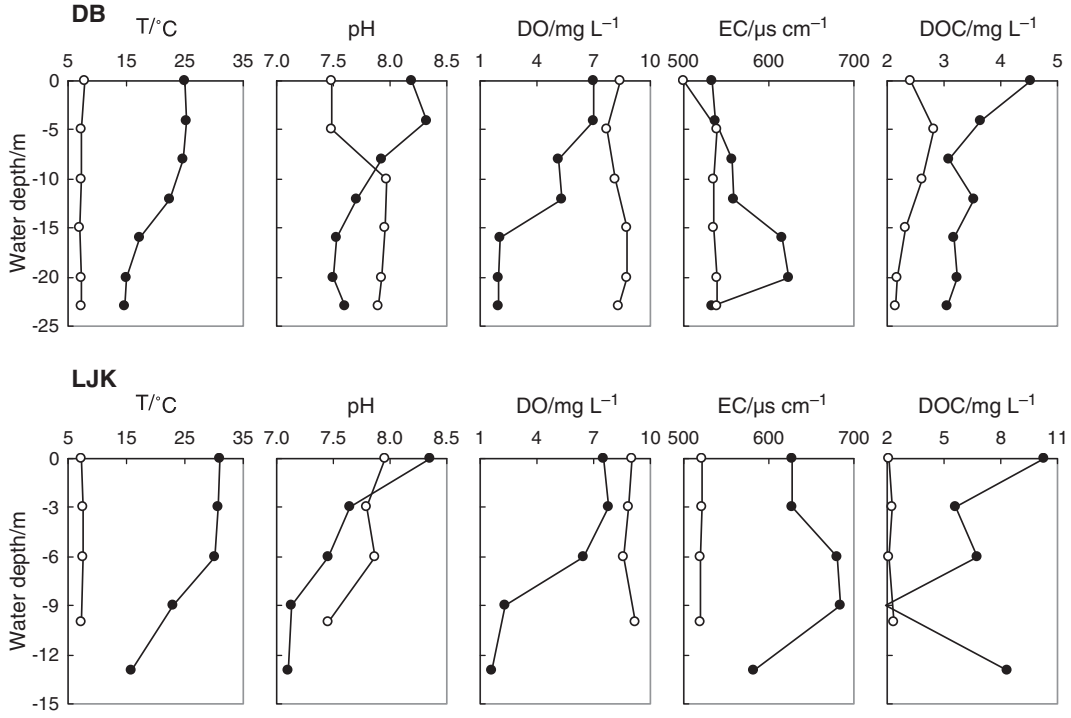

Fig. 2. Plots of environmental parameters for DB and LJK stations of Aha Lake. For DB station, closed circles refer to data of August 2006, while open circles refer to data of January 2007. For LJK station, closed circles refer to data of July 2006, while open circles refer to data of January 2007.

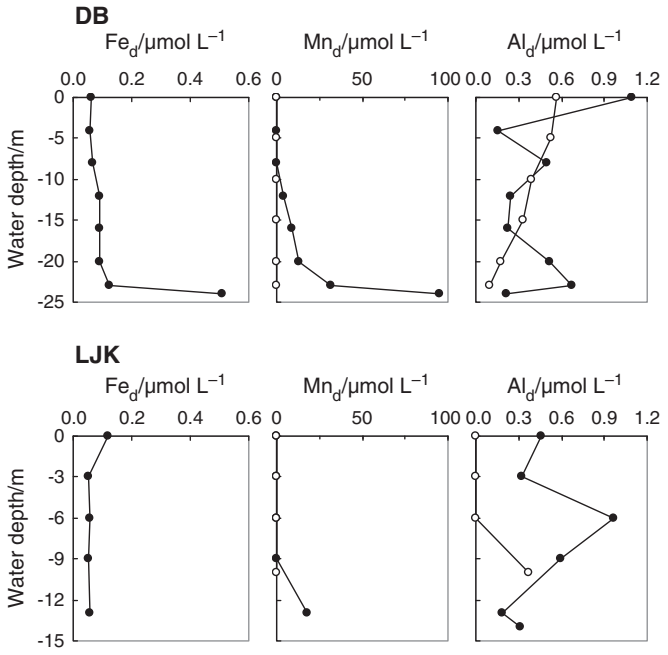

Fig. 3. Plots of dissolved Fe, Mn and Al for DB and LJK stations of Aha Lake. For DB station, closed circles refer to data of August 2006, while open circles refer to data of January 2007. For LJK station, closed circles refer to data of July 2006, while open circles refer to data of January 2007.

3.3. Fe isotopic compositions, Fe, Mn, and Al concentrations of suspended particulate

Fe, Mn, and Al concentrations and Fe isotope data of the SPM samples are summarized in Table 2. Two aerosol samples were also measured for their Fe isotopic compositions (Table 2). The dissolved iron was not analyzed for Fe isotopes because of its low concentration (Fig. 3).

3.3.1. Riverine SPM

Fe, Mn and Al concentrations of SPM samples varied significantly among different rivers within different seasons. YR had a Fe concent of 2199.42 μg L^{-1} in winter, much higher than those of other rivers (46.81–170.71 μg L^{-1}) (Table 2). YR, CR and BR also displayed much higher Mn contents than other inflowing rivers. Significant decreases were clearly observed for both Fe and Mn in CR, LR and BR when water flow decreases in winter (Table 2). The particulate Al contents of the rivers were largely variable, higher in summer than in winter.

The Fe, Mn contents were normalized to Al to determine their enrichment as relative to Al. Fe/Al ratio can be used as indicators of detrital or non-detrital inputs of Fe by comparing with the detrital background ratios (Lyons et al., 2003; Lyons and Severmann, 2006; Fehr et al., 2008). Rivers that are not contaminated with polluted drainages near Guiyang were measured as the background data with Fe/Al ratios of 0.30 to 0.37 (not shown in the table). The atmospheric particles also had similar Fe/Al ratios of 0.37 to 0.39. YR, CR and BR had Fe/Al ratios ranging from 0.63 to 7.36, much higher than those of the

Table 2
Iron isotopic compositions, chemical composition of trace ions Fe, Mn and Al of Aha Lake and its inflowing rivers.

Sample station	Date	Depth (m)	δ^{56}Fe (‰)	δ^{57}Fe (‰)	Fe (μg L^{-1})	Mn (μg L^{-1})	Al (μg L^{-1})	Fe/Al	Mn/Al
DB	Aug 2006	0	−0.16	−0.25	21.99	9.86	31.69	0.33	0.15
DB	Aug 2006	−8	−0.10	−0.13	6.54	6.19	8.11	0.39	0.37
DB	Aug 2006	−12	−0.41	−0.52	9.62	114.04	11.55	0.40	4.85
DB	Aug 2006	−16	−0.84	−1.25	12.50	272.57	8.94	0.67	14.97
DB	Aug 2006	−20	−0.70	−1.02	15.98	430.51	14.86	0.52	14.23
DB	Aug 2006	−23	−0.60	−0.95	16.02	424.97	14.81	0.52	14.09
DB	Aug 2006	−24	−0.53	-0.73					
LJK	July 2006	0	−0.42	−0.65	7.53	5.63	6.89	0.53	0.40
LJK	July 2006	−3	−0.26	−0.44	8.40	7.07	5.65	0.72	0.61
LJK	July 2006	−6	−0.31	−0.46	28.75	63.18	12.65	1.10	2.45
LJK	July 2006	−9	−0.33	−0.43	36.36	61.02	21.38	0.82	1.40
LJK	July 2006	−13	−1.36	−1.98	43.86	417.10	16.00	1.32	12.80
LJK	Oct 2006	−14	−0.32	−0.47					
DB	Jan 2007	0	−0.09	−0.17	26.48	14.30	32.44	0.39	0.22
DB	Jan 2007	−5	−0.07	−0.07	45.84	23.85	52.61	0.42	0.22
DB	Jan 2007	−10	−0.18	−0.24	27.80	25.33	32.71	0.41	0.38
DB	Jan 2007	−15	−0.30	−0.45	12.58	15.02	16.51	0.37	0.45
DB	Jan 2007	−20	−0.24	−0.31	19.63	23.70	22.22	0.43	0.52
DB	Jan 2007	−23	−0.14	−0.18	12.62	17.51	13.19	0.46	0.65
LJK	Jan 2007	0	−0.21	−0.33	9.10	14.63	9.79	0.45	0.73
LJK	Jan 2007	−3	−0.22	−0.32	17.10	25.33	17.74	0.46	0.70
LJK	Jan 2007	−6	−0.26	−0.38	12.11	23.20	14.41	0.41	0.79
LJK	Jan 2007	−10	−0.22	−0.36	11.30	21.83	13.44	0.41	0.80
YR	Aug 2006	0	−0.38	−0.56					
YR	Jan 2007	0	−0.03	−0.06	2199.42	251.67	144.06	7.36	0.86
CR	Aug 2006	0	−0.49	−0.73	234.21	105.77	165.49	0.68	0.31
CR	Jan 2007	0	−0.35	−0.52	46.81	11.79	11.41	1.98	0.51
LR	Aug 2006	0	−0.16	−0.23	410.94	16.10	634.88	0.31	0.01
LR	Jan 2007	0			170.71	2.76	191.89	0.43	0.01
BR	Aug 2006	0	−0.88	−1.29	329.44	107.70	135.27	1.17	0.39
BR	Jan 2007	0	−0.13	−0.22	106.71	15.81	81.56	0.63	0.10
SR	Aug 2006	0	0.07	0.05					
SR	Jan 2007	0	−0.12	−0.16	125.39	14.47	142.79	0.42	0.05
XR	Aug 2006	0	−0.58	−0.84	13.71	234.30	6.22	1.06	18.50
XR	Jan 2007	0	−0.28	−0.45	32.59	34.58	30.64	0.51	0.55
Aerosol-1	Oct 2006		0.08	0.14				0.37	0.01
Aerosol-2	Oct 2006		0.12	0.17				0.39	0.03

Iron isotope data are reported as δ^{x}Fe relative to IRMM-014, and all the data are an average of duplicate analyses.

background rivers. And these rivers also have higher Mn/Al ratios of 0.10 to 0.86. As the only outflow river, XR also displayed an enrichment of Fe and Mn relative to Al especially in summer (Table 2). In contrast, the average Fe/Al and Mn/Al ratios of LR and SR were only 0.39 and 0.02, respectively.

The studied riverine samples have δ^{56}Fe values of −0.88‰ to 0.07‰, which are isotopically light relative to igneous rocks (δ^{56}Fe = 0.09‰, Beard et al., 2003a). Within the inflowing tributaries, YR, CR, and BR tend to have very light iron isotopic compositions ranging from −0.88‰ to −0.38‰ in summer (Table 2). With the decline of water flow in winter, significant increases in δ^{56}Fe values were clearly observed for YR (−0.03‰) and BR (−0.13‰) (Fig. 1). In contrast, there is only a slight increase for CR, varying from −0.49‰ to −0.35‰. Besides, XR had a similar seasonal variation trend with YR and BR, increasing from −0.58‰ (summer) to −0.28‰ (winter).

3.3.2. Lake SPM

Concentrations of Fe, Mn and Al in lake SPM were respectively 6.54–43.86 μg L^{-1}, 5.63–430.5 μg L^{-1}, and 5.65–31.7 μg L^{-1}, in summer, and generally higher than those in winter (Table 2), significantly lower than those in the riverine SPM. Depth-dependent distributions of Fe and Mn concentrations, Fe/Al and Mn/Al ratios are displayed in Figs. 4 and 5, respectively. At DB station, the Fe contents did not show a clear depth-dependent relationship, but the Mn contents showed a significant increase from 10 m depth to the bottom in summer. The contents of both Fe and Mn increased with the depth of the water column. In Fig. 5, the Fe/Al, Mn/Al ratios of Lake SPM at DB station were homogenous or with slight variations throughout the water column in winter, while in summer, there were significant increases especially for particles near the redox boundary (Fig. 5).

Similar to riverine SPM samples, Lake suspended particle samples also have negative δ^{56}Fe values, with a range of −1.36‰ to −0.10‰ in summer and −0.30‰ to −0.07‰ in winter (Table 2). In winter, the bottom samples of DB station have a mean iron isotopic composition

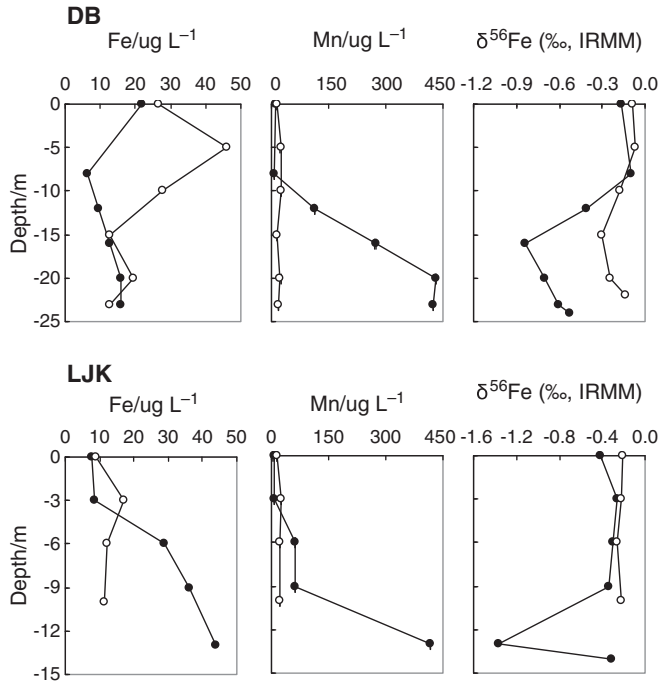

Fig. 4. Depth profiles of Fe, Mn and δ^{56}Fe values of suspended particulate matter. For DB station, closed circles refer to data of August 2006 and open circles refer to data of January 2007. For LJK station, closed circles refer to data of July 2006 and open circles refer to data of January 2007, and the SPM at 14 m depth was collected in October 2006.

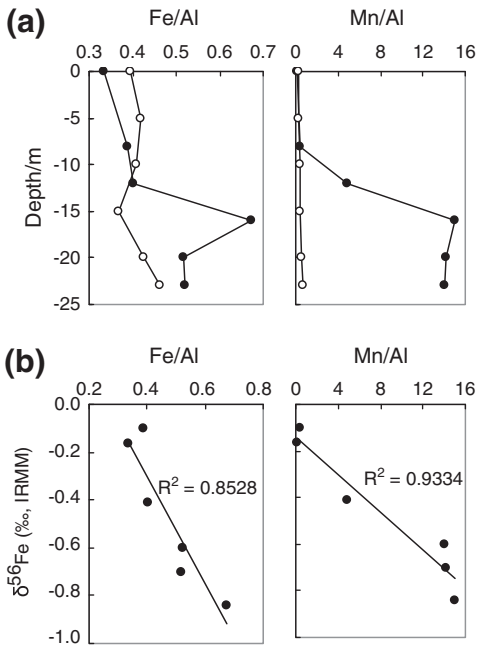

Fig. 5. (a) Depth profile of Fe/Al and Mn/Al for suspended particles of DB station. Closed circles refer to data of August 2006 and open circles refer to data of January 2007. (b) Correlations between δ^{56}Fe values and the corresponding Fe/Al and Mn/Al ratios of DB station.

of −0.23‰, slightly lighter than the surface ones. While at LJK station, all the lake SPM samples are indistinguishable from each other within uncertainties although they all are still isotopically lighter (Fig. 4). During summer stratification, the surface sample of LJK station has a δ^{56}Fe value of −0.42‰ which is significantly lighter than that in winter (−0.21‰) (Table 2 and Fig. 4). Except for the epilimnetic sample, other SPM samples in the oxygenated water column seem to have similar isotopic compositions with an average δ^{56}Fe of −0.30‰, which are similar with those in winter (−0.23‰). In contrast, there is only very slight drop for the epilimnetic SPM in summer (−0.16‰) with respect to that in winter (−0.09‰) at DB station (Table 2 and Fig. 4).

A pronounced decrease of δ^{56}Fe was clearly observed for both DB and LJK stations with the increase of water depth until the minimum δ^{56}Fe values of −0.84‰ and −1.36‰ are reached near the redox boundary (Fig.4), where the maximum Fe/Al and Mn/Al ratio was also displayed. From that depth, we observed an increase of δ^{56}Fe from −0.84‰ to −0.53‰ until the water–sediment interface, which is to some extent similar with that reported by Malinovsky et al. (2004). Comparing with the sample at 13 m depth of LJK station in July 2006, the suspended particles sampled near water–sediment interface in October 2006 at LJK station have a much heavier isotopic composition of −0.32‰ (Fig. 4 and Table 2), which suggests that a similar increase of δ^{56}Fe seemed to occur at LJK after the minimum value since water stratification will last until overturn mixing at the end of autumn.

4. Discussion

4.1. Thermal and chemical stratification of Aha Lake

During summer stratification, the changes of geochemical characteristics throughout the water column seem to indicate that respiration processes control the chemical compositions of deep water strata (e.g., low pH, low DO, high DOC and high EC), while fluvial inputs and primary production processes lead to high pH, high DO, and high DOC in epilimnion (Fig. 2). DOC concentrations are controlled by both natural and anthropogenic inputs and autochthonous processes as well (Sachse

et al., 2005). During high-flow period, lake water discharge is high, which makes allochthonous inputs become increasingly important especially as Aha Lake is a narrow water system. Concurrently with the high concentration of DOC in surface lake water (Fig. 2), the dissolved aluminum was also high in summer (Fig. 3), indicating that epilimnion is significantly influenced by fluvial inputs. The high concentration of dissolved Fe in epilimnion at LJK is attributed to the high content of DOC (Figs. 2 and 3), which favors the formation of soluble iron–organic complexes or small iron particles stabilized by adsorption onto humic matter (Perdue et al., 1976; Koenings, 1976; Cameron and Liss, 1984; Tipping et al., 2002). The water samples were filtered with 0.45 μm filters and so, a considerable part of "dissolved" fraction is probably colloid Fe, as predicted by Björkvald et al. (2008).

The deep water strata were characterized by lower and depth-decreasing dissolved oxygen, higher and depth-increasing EC, and higher DOC as well, implying that degradation of organic matter prevailed in the bottom. The sudden increase of DOC in the near-sediment water of the LJK water coulmn may be influenced by the sediment–water fluxes (Fig. 2). With the depletion of dissolved oxygen, the degradation of organic matter is coupled with a succession of reductive dissolutions using Fe oxides/hydroxides or Mn oxide/hydroxides as electron acceptors (Stumm and Morgan, 1981). These processes have been widely described in lakes (Balistrieri et al., 1992; 1994; Davison, 1993; Nealson and Saffarini, 1994; Zaw and Chiswell, 1999; Bellanger et al., 2004). The increases of Fe and Mn in the bottom strata of Aha Lake may also be due to the reductive dissolution of particulate matter (Fig. 3). However, the increase of dissolved Fe is not as strong as dissolved Mn, indicating that Mn oxides, as the more active electron acceptor (Stumm and Morgan, 1981), are preferentially involved into redox transformations. It is also possible that some dissolved Fe was oxided by Mn(IV) or be scavenged by formation of Fe sulfides (Davison and De Vitre, 1992). The strong increase of dissolved Fe and Mn near water–sediment interface may result from sediment–water diffusion during water stratification.

4.2. Seasonal variation in δ^{56}Fe values of riverine SPM

Except for the SPM in SR, all of the SPM samples collected from the tributaries show lower δ^{56}Fe values in summer than in winter. For the heavily contaminated rivers BR and YR by coal mining, the δ^{56}Fe values of the SPM were 6–10 times lower in summer than in winter. The Fe/Al concentration ratios of the riverine SPM samples were variable but all were remarkably higher than those of the studied SPM of the background rivers. The seasonal variation in δ^{56}Fe value of the riverine SPM should be ascribed to the change in source of Fe and geochemical process in the watershed.

YR and BR are heavily contaminated by coal mine drainages, and hence their particulate Fe is supposed to be mainly originated from weathering of pyrite mineral in coal-containing strata. δ^{56}Fe value is reflective of Fe oxides/hydroxides after oxidation of pyrite, numerous studies have been carried out on iron isotopic compositions of pyrite and a variable range of −3.5‰ to +1.2‰ was reported for the pyrite, which has been summarized in Fehr et al. (2008), Roger et al. (2008) and Egal et al. (2008). According to Egal et al. (2008), pyrite has lower δ^{56}Fe values than Fe oxides at the same site although pyrite is theoretically expected to have heavier isotopes relative to most other Fe oxides (Polyakov and Mineev, 2000). In this study, we only got δ^{56}Fe values of −0.88‰ to −0.03‰ for suspended particles of these two rivers, but no data of the starting pyrites. So, detailed studies need to be done for further discussions.

Microbial-induced pyrite oxidation produces little iron isotope fractionation (Roger et al., 2008). Whereas, it is suggested by Balci et al. (2006) that precipitations tend to have lighter δ^{56}Fe (−1.46‰ to −0.04‰) than coexisting $Fe(III)_{aq}$ in synthetic acidic ferric sulfate solutions. Skulan et al. (2002) reported an equilibrium fractionation factor ($\Delta^{56}Fe_{Fe(III)\text{-hematite}}$) of −0.10‰ with long-term experiment and a kinetic fractionation factor of 1.32‰ with short-term experiment. In summer, large amount of AMD was produced with high water flow. While in winter, water flow decreases dramatically and the acidophilic iron-oxidizing bacteria may also be less active under lower temperature. As a result, there would be enough time for aqueous and solid phases to be equilibrated. So, the big seasonal variations especially observed for the YR and BR are expected to be explained by the differences between equilibrium and kinetic fractionation. In addition, the difference between sources of particulate Fe in winter and summer was responsible for the seasonal variations in Fe isotopic composition of the SPM, since there should be more Fe particle from oxidation of pyrite in summer than in winter.

According to Brantley et al. (2001; 2004), Fe dissolved from the silicate mineral by siderophore-producing bacteria has an isotopic composition of 0.8‰, lighter than the bulk mineral. Besides, negative shifts of ca. 0.6‰–1‰ were observed between the exchangeable Fe of the studied soil and the hornblende or Fe oxyhydroxides. The organically chelated Fe in the O and E horizons of the soil profile is also found to have lighter δ^{56}Fe (Fantle and Depaolo, 2004; Emmanuel et al., 2005). Ingri et al. (2006) reported that it is just the organically bounded Fe that provides river particulates with the lighter iron isotopes during high water discharge period. They also showed that the drop in δ^{56}Fe was closely correlated with the increases of both dissolved Al and TOC concentrations. In summer, more particulate Fe is derived from soil weathering than in winter, since river water is mainly recharged by runoff in summer. Accordingly, the lower δ^{56}Fe values for most of riverine SPM should result from more particulate Fe from weathering of soil in summer than in winter.

No significant seasonal variation was observed for CR (Fig. 1 and Table 2). The difference may be linked to another contamination by sewage characterized with high concentrations of DOC, NO_3^-, Cl^- and low SO_4^{2-} (Table 1). LR and SR are contaminated with only sewage and they had Fe/Al ratios similar to bulk shales and Mn/Al ratios of only 0.01 to 0.05. Their δ^{56}Fe values ranged from −0.16‰ to 0.07‰ (Table 2). As the only outflow river, XR has a temperature of 12.0 °C in summer, which indicates that the water is from the bottom of Aha Lake. And a lighter δ^{56}Fe of −0.58‰, being similar to that of SPM in bottom strata, further confirms the source of iron in XR. However, SPM in XR had higher Fe/Al and Mn/Al ratios than bottom strata due to the increase of oxygen in river water. The lower iron isotopic compositions and seasonal variations are expected to be derived from biogeochemical processes in bottom strata.

4.3. Source controls on the iron isotope composition of SPM in the lake

SPM in lake water is mainly supplied by fluvial input and atmospheric deposition (allochthonous material), materials produced within the lake (autochthonous material) and sediment resuspension (Håkanson and Peters, 1995). Aha Lake has a surface area of only 4.5 km^2, a water depth of 14–24 m as well as temperature gradients of >10 °C during summer stratification (Fig. 2), which implies that wind induced resuspension of sediment will have limited contributions. Atmospheric dust is known as one of the main Fe sources for oceans (Jickells et al., 2005) and sometime the atmospheric Fe load is of the same magnitude as fluvial input for lakes although the particles seem to have small impact on Fe behavior in lakes (Shaked et al., 2004; Herut et al., 2001). Two aerosol samples have been also analyzed for their δ^{56}Fe values, and the analyzed δ^{56}Fe values ranged from 0.08‰ to 0.12‰ (Table 2), which are similar to those of igneous rocks but slightly heavier than Dunhuang samples (−0.16‰ to −0.10‰) (Beard et al., 2003b). As compared to the SPM both in the tributaries and lake, the aerosols showed significantly higher δ^{56}Fe values. Whereas the surface water of the lake showed higher δ^{56}Fe values in both winter and summer than deep water and inflowing river water in summer as well, contribution of aerosols to the high δ^{56}Fe values of the surface water is possible. However, it is impossible at present to quantify the atmospheric contribution because no flux of particulate Fe is available. Aha Lake is a

highly mineralized reservoir with low concentrations of Chlorophyll-a (6.08 μg L^{-1} to 6.63 μg L^{-1}). As a result, it is considered that the fluvial inputs of SPM, instead of algae production, may play an important role.

River-borne particulate Fe is mainly in the form of oxides or iron associated clay minerals and organically bounded Fe as well. Clay minerals will sink quickly, leaving lighter amorphous oxides to be the dominant Fe-bearer in surface lake water (Davison, 1993). In general, the river water samples had much higher particulate Fe contents than lake water samples, which suggests that most particles were settled down after being transported into the lake and/or during river water–lake water mixing. During settlement of particles in lake or estuary, fractionation of Fe isotopic composition of SPM may take place due to size separation and sorption/desorption processes, but it is not easy to constrain. The suspended particle in surface water sampled at LJK station has a δ^{56}Fe value of −0.42‰ and the corresponding Fe/Al is 0.53, comparable with those of the rivers YR and CR. LR is a small river seriously contaminated with sewage and has an iron isotopic composition of −0.16‰ associated with a Fe/Al of only 0.31. CR has δ^{56}Fe value of −0.49‰ and the Fe/Al ratio of 0.68, which are similar to those of epilimnetic particles at LJK in summer. So, CR may be considered to be a significant contributor in the drop of epilimnetic δ^{56}Fe. However, the epilimnetic concentrations of DOC (10.26 mg L^{-1}) and dissolved Al (12.30 μg L^{-1}) are all high at LJK station (Figs. 2 and 3). Its DOC concentration is higher than both the inflowing rivers (1.96 mg L^{-1} to 7.84 mg L^{-1}) and DB station (4.54 mg L^{-1}) although they have similar primary productions. This suggests that there are other possible sources depleted in ^{56}Fe.

Aha Lake is an artificial reservoir with a narrow and long water surface. It is possible for the movable fractions in the O or E horizons of the soil to flush into lake with the high water discharge during summer peak flow period. This can be indicated by the much higher DOC concentration in summer than in winter. The organically bounded Fe did not easily settle down quickly during summer stratification. Therefore, Fe–C colloids seem to be another contributor for the lighter δ^{56}Fe values of epilimnetic particles at LJK in summer.

4.4. The "ferrous wheel" and depth-related variations of iron isotopic composition

As shown in Fig. 4, significant depth-related variations of δ^{56}Fe were clearly observed for both DB and LJK stations during summer. There is a minimum δ^{56}Fe of −1.36‰ appeared near redox boundary at LJK (Table 2), being much lighter than that of fluvial inputs and aerosol depositions. In contrast, homogenous water columns were displayed in winter. It is suggested that autochthonous materials produced within biogeochemical processes are important in controlling iron isotope compositions of SPM especially in the bottom strata.

During summer stratification, DO is sufficiently removed from the bottom strata of Aha Lake and a pseudo redox boundary is established over the hypolimnion. According to the conceptual model of Fe transport near the redox boundary (Davison, 1985; Davison and De Vitre, 1992), there is a ready interconversion between the defined active iron oxides and the reduced $Fe(II)_{aq}$ (Fig. 6). The suspended solids were continuously supplied to the redox boundary and the reactive Fe fractions were accordingly reduced. There is a point source of $Fe(II)_{aq}$ formed near the boundary. The reduced $Fe(II)_{aq}$ can diffuse up into the oxidizing zone or down into deep reducing zone. The dissolved $Fe(II)_{aq}$ will be re-oxidized to particulate oxides when it encounters the oxidants. The re-oxidized fractions will sink back into the reducing zone or diffuse upwardly. Consequently, the so called "ferrous wheel" (Campbell and Torgersen, 1980) is established near the redox boundary (Fig. 6). Such kind of iron recycling is expected to be active in Aha Lake as there were important reactive iron oxides continuously supplied to this well stratified water system with fluvial inputs, although large amount of the particulates settled down during river water–lake water mixing.

During cycling of iron, heavy iron isotopes generally tend to accumulate preferentially in ferric Fe phases (Polyakov and Mineev, 2000; Beard and Johnson, 2004). Both of dissimilatory iron reduction (DIR) and abiotic reductive process yielded significant iron isotope fractionation with $\Delta^{56}Fe_{Fe(II)aq-Fe(III)oxide}$ of ca. −1.3‰ in experimental studies (Beard et al., 1999; 2003a; Johnson et al., 2005; Bullen et al., 2001). In natural systems, light iron isotope compositions of porewaters and lake water in reduced environments were all attributed to DIR processes (Severmann et al., 2006; 2008; 2010; Teutsch et al., 2009). In the bottom strata of Aha Lake, microbial iron reduction may be also important even if nitrate or Mn(IV) existed in the water column, as strong enrichments of iron were clearly observed (Fig. 5). Additionally, good negative correlation between δ^{56}Fe values and Fe/Al ratios implies an iron source depleted in ^{56}Fe was produced with similar iron reduction processes in bottom strata and sediments (Fig. 5).

In air-saturated water, $Fe(II)_{aq}$ will be oxidized rapidly at a pH value of 7–8 and a temperature of 10 °C (Davison and De Vitre, 1992). Aha Lake had a pH value of 7.1 to 7.5 with a water temperature of ca. 16 °C in the bottom. Hence the upwardly diffusing $Fe(II)_{aq}$ will be oxidized rapidly and almost quantitatively by dissolved oxygen or Mn(IV) and little fractionation will be expected. Moreover, the aggregation of Fe oxides especially the neo-formed Fe colloids is slow (Laxen and Chandler, 1983; Davison and De Vitre, 1992), suggesting that the residence time of Fe oxides with low δ^{56}Fe values will be sufficiently long to be the instantaneously dominant species even though they will eventually settle down to sediment. An enrichment of reactive iron, with approximately a Gaussian shape as described in Davison and De Vitre (1992), is consequently observed with the repetitive Fe cycling (Fig. 6). An approximate symmetrical Gaussian shape of Fe/Al developed at DB station (Fig. 5). These suggest that "ferrous wheel" plays an important role in decreasing δ^{56}Fe values of lake SPM near the redox boundary. A more variable range of δ^{56}Fe (−1.36‰ to −0.26‰) was observed at LJK (Fig. 4 and Table 2), which can be probably explained by the larger amount of fluvial inputs of reactive iron (Table 2 and Fig. 1).

According to Severmann et al. (2008), there is a benthic Fe shuttle from oxic shelf to euxinic basin. In the conceptual model of lacustrine system, each deep stratum was thought to be completely mixed as the lateral rate of transport is several orders of magnitude higher than that of vertical transport (Davison et al., 1982; Davison, 1993). So, only the net vertical transport was considered here. In addition to the source $Fe(II)_{aq}$ produced within the reductive dissolution of both fluvial and incoming reactive Fe(III), sediment–water diffusion may also do some contribution to Fe enrichment in bottom strata. However, it is not expected to be important as the concentration of dissolved Fe was not high except one sample collected near sediment (Fig. 3). Even if there were sediment–water Fe fluxes, the dissolved Fe may be oxided by the large amount of Mn(IV) (Fig. 4). Mn(IV) oxides were also considered as important oxidants near redox boundary, which can be presumably known from the good negative relationship between δ^{56}Fe and Mn/Al (Fig. 5).

A rough calculation was conducted in order to evaluate the reactive iron produced within the repetitive Fe cycling. The particulates were roughly considered to be composed of autochthonous inputs (newly-formed Fe oxides on site) and allochthonous inputs (riverine and atmospheric inputs). The percentage of autochthonous reactive Fe(III) was roughly calculated using this formula:

$$\delta^{56}Fe_{SPM} = \delta^{56}Fe_{allo}\ (1-f) + \delta^{56}Fe_{auto}\ f$$

$$\delta^{56}Fe_{auto} = \Delta^{56}Fe + \delta^{56}Fe_{SRM}$$

$$\delta^{56}Fe_{SRM} = \delta^{56}Fe_{YR}\ J_{YR} + \delta^{56}Fe_{CR}\ J_{CR} + \delta^{56}Fe_{BR}\ J_{BR}$$

where $\delta^{56}Fe_{allo}$ strands for δ^{56}Fe value of allochthonous inputs, $\delta^{56}Fe_{auto}$ for δ^{56}Fe value of autochthonous reactive Fe(III), $\delta^{56}Fe_{SRM}$

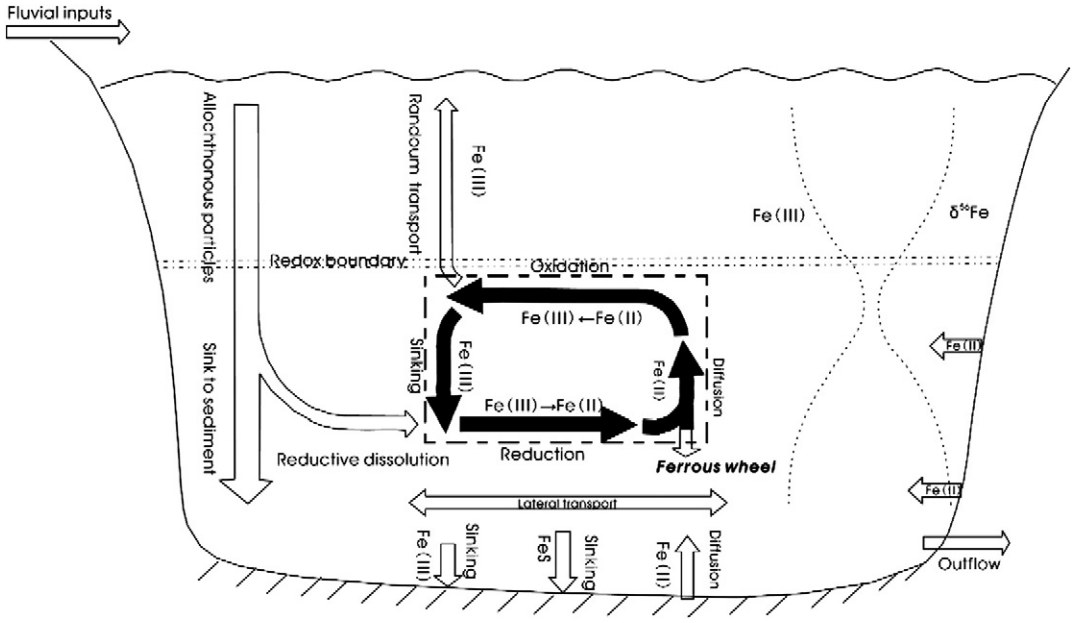

Fig. 6. The "ferrous wheel" near redox boundary (modified from Davison, 1985, 1993).

for starting reactive Fe oxides, $\delta^{56}Fe_i$ and J_i respectively for the Fe isotope composition and ratio of particulate Fe flux of river i to the total particulate Fe flux of the rivers YR, CR and BR, and f for its percentage in the sampled particulates. We take roughly average $\delta^{56}Fe$ values of epilimnetic particulates as those ($\delta^{56}Fe_{allo} = -0.16‰$ for DB station, $\delta^{56}Fe_{allo} = -0.34‰$ for LJK station) of allochthonous inputs including atmospheric and riverine inputs. The weighted average $\delta^{56}Fe$ value (−0.38‰) of YR, CR and BR, all of which are polluted by coal mining in the watershed and showed high Fe/Al ratios, is considered as the starting reactive Fe oxides ($\delta^{56}Fe_{SRM}$). A fractionation factor of −1.3‰ ($\Delta^{56}Fe_{Fe(II)aq-Fe(III)oxide}$) was used (Beard et al., 1999; 2003a; Johnson et al., 2005) to calculate the $\delta^{56}Fe$ value of autochthonous reactive Fe(III). Therefore we can obtain a 45% of autochthonous (newly-formed) Fe oxides produced at 16 m depth of DB station within the cycle and 76% at 13 m depth of LJK.

5. Conclusion

This study describes seasonal variations of $\delta^{56}Fe$ values for both lake SPM and riverine particulates. Rivers seriously contaminated with coal mine drainages demonstrate significant enrichment of SO_4^{2-}, Fe and Mn, and a big difference of $\delta^{56}Fe$ between summer and winter. In contrast to the homogenous water column in winter, significant depletions of ^{56}Fe for lake SPM were displayed in both epilimnion and bottom strata during summer stratification.

It is suggested that the ^{56}Fe-depleted iron isotope compositions of particles in lake water during summer are controlled by both tributary inputs, organically-bonded Fe colloids leached from O and E horizons within peak water discharge and biogeochemical processes involved in Fe transformation. The lower $\delta^{56}Fe$ values in deep strata were attributed to 'ferrous wheel' cycling near the redox boundary in stratified Aha Lake. The repetitive cycling was primed with microbial reductive dissolution of the continual supply of fluvial reactive Fe oxides and the newly-incoming Fe oxides. As a result of the Fe recycling and random transport, the newly-formed Fe particles were of approximately a Gaussian shape characterized with depleted ^{56}Fe and elevated Fe/Al ratio. The good negative relationship between $\delta^{56}Fe$ and Fe/Al ratios further revealed that they two together can be considered as good indicators of redox-driven Fe transportation.

Acknowledgements

We thank Xiaolong Liu, Hu Ding and Wei Zhang for their involvement in filed works. This study benefited greatly from discussions with Franck Poitrasson, Peter Dillon, and Jiubin Chen. Two anonymous reviewers and the editor Bernard Bourdon are much appreciated with their thoughtful reviews. This research was financially supported by the Natural Science Foundation of China (Nos. 90610037, 40721002, 40903008 and 40331005).

References

Balci, N., Bullen, T.D., Witte-Lien, K., Shanks, W.C., Motelica, M., Mandernack, K.W., 2006. Iron isotope fractionation during microbially stimulated Fe(II) oxidation and Fe(III) precipitation. Geochim. Cosmochim. Acta 70 (3), 622–639.
Balistrieri, L.S., Murray, J.W., Paul, B., 1992. The cycling of iron and manganese in the water column of Lake Sammamish. Washington. Limnol. Oceanogr. 37, 510–528.
Balistrieri, L.S., Murray, J.W., Paul, B., 1994. The geochemical cycling of trace elements in a biogenic meromictic lake. Geochim. Cosmochim. Acta 58 (19), 3993–4008.
Beard, B.L., Johnson, C.M., 2004. Fe isotope variations in the modern and ancient Earth and other planetary bodies, in: Geochemistry of non-traditional stable isotopes. Rev. Earth. Pl. Sc. 55, 319–357.
Beard, B.L., Johnson, C.M., Cox, L., Sun, H., Nealson, K.H., Aguilar, C., 1999. Iron isotope biosignatures. Science 285, 1889–1892.
Beard, B.L., Johnson, C.M., Skulan, J.L., Nealson, K.H., Cox, L., Sun, H., 2003a. Application of Fe isotopes to tracing the geochemical and biological cycling of Fe. Chem. Geol. 195, 87–117.
Beard, B.L., Johnson, C.M., Von Damm, K.L., Poulson, R.L., 2003b. Iron isotope constraints on Fe cycling and mass balance in oxygenated Earth oceans. Geology 31, 629–632.
Bellanger, B., Huon, S., Steinmann, P., Chabaux, F., Velasquez, F., Vallès, V., Arn, K., Clauer, N., Mariotti, A., 2004. Oxic–anoxic conditions in the water column of a tropical freshwater reservoir (Peña-Larga dam, NW Venezuela). Appl. Geochem. 19, 1295–1314.
Bergquist, B.A., Boyle, E.A., 2006. Iron isotopes in the Amazon River system: weathering and transport signatures. Earth Planet. Sci. Lett. 248, 54–68.
Björkvald, L., Buffam, I., Laudon, H., Mörth, C.-M., 2008. Hydrogeochemistry of Fe and Mn in small boreal streams: the role of seasonality, landscape type and scale. Geochim. Cosmochim. Acta 72 (12), 2789–2804.
Brantley, S.L., Liermann, L., Bullen, T.D., 2001. Fractionation of Fe isotopes by soil microbes and organic acids. Geology 29, 535–538.
Brantley, S.L., Liermann, L.J., Guynn, R.L., Anbar, A., Icopini, G.A., Barling, J., 2004. Fe isotopic fractionation during mineral dissolution with and without bacteria. Geochim. Cosmochim. Acta 68 (15), 3189–3204.
Bullen, T.D., White, A.F., Childs, C.W., Vivit, D.V., Schultz, M.S., 2001. Demonstration of significant abiotic iron isotope fractionation in nature. Geology 29, 699–702.
Cameron, A.J., Liss, P.S., 1984. The stabilization of "dissolved" iron in freshwaters. Water Res. 18, 179–185.

Campbell, P., Torgersen, T., 1980. Maintenance of iron meromixis by iron redeposition in a rapidly flushed Monimolimion. Can. J. Fish. Aquat. Sci. 8, 1303–1313.
Clasen, J., Bernhardt, H., 1974. The use of algal assays for determining the effect of iron and phosphorus compounds on the growth of various algal species. Water Res. 8, 31–44.
Coale, K.H., Fitzwater, S.E., Gordon, R.M., Johnson, K.S., Barber, R.T., 1996. Control of community growth and export production by upwelled iron in the equatorial Pacific Ocean. Nature 379, 621–624.
Davison, W., 1985. Conceptual models for transport at a redox boundary. In: Stumm, W. (Ed.), Chemical Processes in Lakes. Wiley Interscience, New York, pp. 31–53.
Davison, W., 1993. Iron and manganese in lakes. Earth Sci. Rev. 34, 119–163.
Davison, W., De Vitre, R., 1992. In: Buffle, J., van Leeuwen), H.P. (Eds.), Iron particles in freshwater. In Environmental Particles 1: 315–355. Lewis Publishers, Chelsea.
Davison, W., Woof, C., Rigg, E., 1982. The dynamics of iron and manganese in a seasonally anoxic lake; direct measurement of fluxes using sediment traps. Liminol. Oceangr. 27 (6), 987–1003.
Egal, M., Elbaz-Poulichet, F., Casiot, C., Motelica-Heino, M., Négrel, P., Bruneel, O., Sarmiento, A.M., Nieto, J.M., 2008. Iron isotopes in acid mine waters and iron-rich solids from the Tinto–Odiel Station (Iberian Pyrite Belt, Southwest Spain). Chem. Geol. 253, 162–171.
Emmanuel, S., Erel, Y., Matthews, A., Teutsch, N., 2005. A preliminary mixing model for Fe isotopes in soils. Chem Geol. 22, 23–34.
Evans, J.C., Prepas, E.E., 1997. Relative importance of iron and molybdenum in restricting phytoplankton biomass in high phosphorus saline lakes. Liminol. Oceangr. 42, 461–472.
Fantle, M.S., DePaolo, D.J., 2004. Iron isotopic fractionation during continental weathering. Earth Planet. Sci. Lett. 228, 547–562.
Fehr, M.A., Andersson, P.S., Håleius, U., Mörth, C.-M., 2008. Iron isotope variations in Holocene sediments of the Gotland Deep. Baltic sea. Geochim. Cosmochim. Acta 72 (3), 807–826.
Håkanson, L., Peters, R.H., 1995. Predictive Limnology Methods for Predictive Modelling. SPC Academic Publishing, Amsterdam, pp. 1–464.
Herut, B., Nimmo, M., Medway, A., Chester, R., Krom, M.D., 2001. Dry atmospheric inputs of trace metals at the Mediterranean coast of Israel (SE Mediterranean): sources and fluxes. Atmos. Environ. 35, 803–813.
Ingri, J., Malinovsky, D., Rodushkin, I., Baxter, D.C., Widerlund, A., Andersson, P., Gustafsson, Ö., Forsling, W., Öhlander, B., 2006. Iron isotope fractionation in river colloidal matter. Earth Planet. Sci. Lett. 245, 792–798.
Jickells, T., An, Z.S., Andersen, K.K., Baker, A.R., Bergametti, G., Brooks, N., Cao, J.J., Boyd, P.W., Duce, R.A., Hunter, K.A., Kawahata, H., Kubilay, N., La Roche, J., Liss, P.S., Mahowald, N., Prospero, J.M., Ridgwell, A.J., Tegen, I., Torres, R.J., 2005. Global iron connections between desert dust, ocean biogeochemistry and climate. Science 308, 67–71.
Johnson, C.M., Beard, B.L., Roden, E.E., Newman, D.K., Nealson, K.H., 2004. Isotopic constraints on biogeochemical cycling of Fe. Rev. Earth. Pl. Sc. 55, 359–408.
Johnson, C.M., Roden, E.E., Welch, S.A., Beard, B.L., 2005. Experimental constraints on Fe isotope fractionation during magnetite and Fe carbonate formation coupled to dissimilatory hydrous ferric oxide reduction. Geochim. Cosmochim. Acta 69 (4), 963–993.
Johnson, C.M., Beard, B.L., Roden, E.E., 2008. The iron isotope fingerprints of redox and biogeochemical cycling in modern and ancient earth. Annu. Rev. Earth Pl. Sc. 36, 457–493.
Koenings, J.P., 1976. In situ experiments on the dissolved and colloidal state of iron in an acid bog lake. Limnol. Oceanogr. 21, 674–683.
Laxen, D.P.H., Chandler, I.M., 1983. Size distribution of iron and manganese species in freshwaters. Geochim. Cosmochim. Acta 47, 731–741.
Lyons, T.W., Severmann, S., 2006. A critical look at iron paleoredox proxies: new insights from modern euxinic marine stations. Geochim. Cosmochim. Acta 70 (23), 5698–5722.
Lyons, T.W., Werne, J.P., Hollander, D.J., Murry, R.W., 2003. Contrasting sulfur geochemistry and Fe/Al and Mo/Al ratios across the last oxic-to-anoxic transition in the Cariaco Station. Venezuela. Chem. Geol. 195, 131–157.
Malinovsky, D., Rodushkin, I., Baxter, D.C., Öhlander, B., Ingri, J., 2004. Fe isotope fractionation during redox cycling of Fe in lake water. Geochim. Cosmochim. Acta 68 (11), A360 (Suppl. 1).
Malmaeus, J.M., Håkanson, L., 2003. A dynamic model to predict suspended particulate matter in lakes. Ecol. Model. 167, 247–262.
Maréchal, C.N., Télouk, P., Albarède, F., 1999. Precise analysis of copper and zinc isotopic compositions by plasma-source mass spectrometry. Chem. Geol. 156, 251–273.
Martin, J.H., 1990. Glacial–interglacial CO_2 change: the iron hypothesis. Paleoceanography 5, 1–13.
Martin, J.H., Gordon, R.M., Fitzwater, S.E., 1991. The case for iron. Limnol. Oceanogr. 6, 1793–1802.
Nealson, K.H., Saffarini, D., 1994. Iron amd manganese in anaerobic respiration: environmental significance, physiology, and regulation. Annu. Rev. Microbiol. 48, 311–343.
Perdue, E.M., Beck, K.C., Reuter, J.H., 1976. Organic complexes of iron and aluminium in natural waters. Nature 260, 418–420.
Poitrasson, F., Viers, J., Martin, F., Braun, J.-J., 2008. Limited iron isotope variations in recent lateritic soil from Nsimi, Cameroon: implications for the global Fe geochemical cycle. Chem. Geol. 253, 54–63.
Polyakov, V.B., Mineev, S.D., 2000. The use of Mössbauer spectroscopy in stable isotope geochemistry. Geochim. Cosmochim. Acta 64 (5), 849–865.
Roger, B., Herbert, J.R., Schippers, Axel, 2008. Iron isotope fractionation by biogeochemical processes in mine tailings. Environ. Sci. Technol. 42, 1117–1122.
Rouxel, O., Fouquet, Y., Ludden, J.N., 2004. Subsurface processes at the Lucky Strike hydrothermal field, Mid-Atlantic Ridge: evidence from sulfur, selenium, and iron isotopes. Geochim. Cosmochim. Acta 68 (10), 2295–2311.
Sachse, A., Henrion, R., Gelbrecht, J., Steinberg, C.E.W., 2005. Classification of dissolved organic carbon (DOC) in river systems: influence of catchment characteristics and autochthonous processes. Org. Geochem. 36, 923–935.
Severmann, S., Johnson, C.M., Beard, B.L., Mcmanus, J., 2006. The effect of early diagenesis on the Fe isotope compositions of porewaters and authigenic minerals in continental margin sediments. Geochim. Cosmochim. Acta 70, 2006–2022.
Severmann, S., Lyons, T.W., Anbar, A., Mcmanus, J., Gwyneth, G., 2008. Modern iron isotope perspective on the benthic iron shuttle and the redox evolution of ancient oceans. Geology 36 (6), 487–490.
Severmann, S., McManus, J., Berelson, W.M., Hammond, D.E., 2010. The continental shelf benthic iron flux and its isotope composition. Geochim. Cosmochim. Acta 74, 3984–4004.
Shaked, Y., Erel, Y., Sukenik, A., 2004. The biogeochemical cycle of iron and associated elements in Lake Kinneret. Geochim. Cosmochim. Acta 68 (7), 1439–1451.
Skulan, J.L., Beard, B.L., Johnson, C.M., 2002. Kinetic and equilibrium Fe isotope fractionation between aqueous Fe(III) and hematite. Geochim. Cosmochim. Acta 66, 2995–3015.
Staubwasser, M., von Blanckenburg, F., Schoenberg, R., 2006. Iron isotopes in the early marine diagenetic cycle. Geology 34, 629–632.
Stumm, W., Morgan, J.J., 1981. Aquatic Chemistry, an Introduction Emphasizing Chemical Equilibria in Natural Waters, second ed. Wiley –Interscience, New York, pp. 1–780.
Tang, S.H., Zhu, X.K., Cai, J.J., Li, S.Z., He, X.X., Wang, J.H., 2006. Chromatographic separation of Cu, Fe and Zn using AG MP-1 anion exchange resin for isotope determination by MC-ICP-MS. Rock Miner. Anaysis 25 (1), 5–8 (in Chinese with English abstract).
Teutsch, N., Schmid, M., Müller, B., Halliday, A.N., Bürgmann, H., Wehrli, B., 2009. Large iron isotope fractionation at the oxic–anoxic boundary in Lake Nyos. Earth Planet. Sci. Lett. 285, 52–60.
Tipping, E., Rey-Castro, C., Bryan, S.E., Hamilton-Taylor, J., 2002. Al(III) and Fe(III) binding by humic substances in freshwaters, and implications for trace metal speciation. Geochim. Cosmochim. Acta 66 (18), 3211–3224.
Zaw, M., Chiswell, B., 1999. Iron and manganese dynamics in lake water. Water Res. 33, 1900–1910.
Zhu, X.K., O'Nions, R.K., Guo, Y., Reynold, B.C., 2000. Secular variation of Fe isotopes in North Atlantic deep water. Science 287, 2000–2002.
Zhu, X.K., Li, Z.H., Zhao, X.M., Tang, S.H., He, X.X., Belshaw, N.S., 2008. High-precision measurements of Fe isotopes using MC-ICP-MS and Fe isotope compositions of geological reference materials. Acta Petrologica Mineralog. 27 (4), 263–272 (in Chinese with English abstract).